A superamplification effect in the detection of explosives by a fluorescent hyperbranched poly(silylenephenylene) with aggregation-enhanced emission characteristics†

Jianzhao Liu,[ab] Yongchun Zhong,[c] Ping Lu,[ab] Yuning Hong,[ab] Jacky W. Y. Lam,[ab] Mahtab Faisal,[ab] Yong Yu,[ab] Kam Sing Wong[c] and Ben Zhong Tang*[abd]

Received 12th February 2010, Accepted 1st March 2010
First published as an Advance Article on the web 11th March 2010
DOI: 10.1039/c0py00046a

Light emission of a hyperbranched poly(silylenephenylene) is quenched exponentially by picric acid, with quenching constant up to ~1.5 × 10^5 L mol^{-1}. This superamplification effect makes the polymer a highly sensitive chemosensor for explosive detection.

Sensors based on fluorescent conjugated polymers (FCPs) have attracted much attention, due to their amplified response and superior sensitivity to analytes, in comparison to their low molar mass congeners.[1] Among many potential applications of FCPs, the detection of explosives is of great current interest because of its anti-terrorism implications.[2] Much effort has been devoted to the development of linear FCPs with an amplification effect for sensitive detection of explosives. It has been shown that a FCP with a fast rate of exciton migration over a long sequence of its repeat units along the one-dimensional (1D) chain affords a high sensitivity (Fig. 1A).[1] The sensing performance of the FCP, however, is often deteriorated by the aggregation of its linear chains. This notorious aggregation-caused quenching (ACQ) effect interferes with the detection of the analytes that induce the polymer chains to aggregate in solutions.

Hyperbranched FCPs are promising candidates for fluorescent sensors for sensitive detection of explosives, because they offer multiple exciton migration channels and diffusion pathways *via* numerous branches in the three-dimensional (3D) space (Fig. 1B). The non-planar globular topological structures of the polymers make their chromophoric repeat units difficult to pack in a compact and ordered fashion and the lack of π–π stacking interaction in the polymer aggregates makes detrimental species such as excimers difficult to form. This is envisaged to help eliminate the ACQ effect as well as the associated false-positive signal generation.

Our groups have discovered an aggregation-induced emission (AIE) effect that is exactly opposite to the ACQ effect discussed above.[3] A series of small compounds that are non-emissive when dissolved as isolated molecules in good solvents are induced to emit efficiently by aggregation as nanoparticles in poor solvents or as films in the condensed phase. A typical example of an AIE-active luminogen is tetraphenylethene, which takes a propeller-shaped conformation. We have proved that the AIE effect is caused by the restriction to intramolecular rotations (RIR) in the luminogen molecules by the aggregate formation, which effectively blocks the non-radiative energy dissipation channels and populates the radiative decay of the excitons.

In our previous work, we have opened a new synthetic route to hyperbranched polyphenylenes through polycyclotrimerization of aromatic diyne monomers.[4] The polymers comprise numerous aromatic branches emanating in the 3D space, whose aggregates are expected to experience little π–π interaction. On the other hand, the intramolecular rotations of the aromatic rings will be restricted when the polymers are aggregated in poor solvents and the activation of the RIR process may boost their emissions in the aggregate state. With these considerations in mind, in this work, we investigated the fluorescence behaviours of a hyperbranched poly(silylenephenylene) (*hb*-PSP; Chart 1)[5] in the solution and aggregate states.

The *hb*-PSP possesses a σ*–π* conjugated structure, arising from the electronic communication between the silicon atoms and the triphenylbenzene (TPB) units, as justified by the red shifts of its absorption and emission peaks from those of TPB by 14 and 24 nm, respectively.[5] As anticipated, aggregate formation plays a constructive, instead of destructive, role in the emission process of the *hb*-PSP.

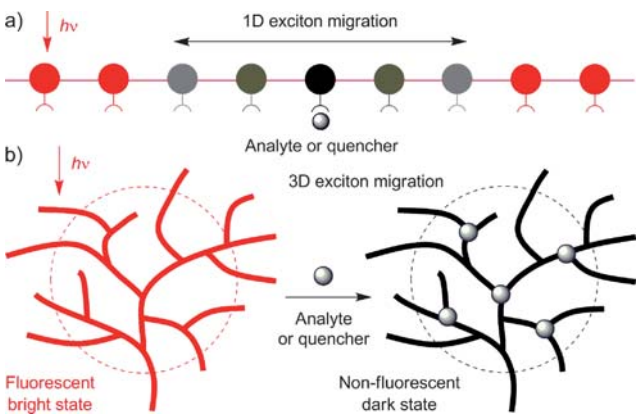

Fig. 1 Schematic illustrations of the amplification effects involved in the quenching processes of the fluorescence from (A) one-dimensional (1D) linear and (B) three-dimensional (3D) hyperbranched polymers by analytes.

[a]*Department of Chemistry, Institute of Molecular Functional Materials, The Hong Kong University of Science & Technology (HKUST), Clear Water Bay, Kowloon, Hong Kong, China. E-mail: tangbenz@ust.hk*
[b]*HKUST Fok Ying Tung Research Institute, Nansha, Guangzhou, China*
[c]*Department of Physics, HKUST, Hong Kong, China*
[d]*Department of Polymer Science & Engineering, Zhejiang University, Hangzhou, 310027, China*

† Electronic supplementary information (ESI) available: Experimental details, absorption spectra of PA and *hb*-PSP and PL spectrum of *hb*-PSP in THF solutions, PL spectra of *hb*-PSP in THF–water mixture (5 : 5 v/v) containing different amounts of PA, and fluorescence decay curves of the THF solutions of *hb*-PSP containing different amounts of PA at 380 nm. See DOI: 10.1039/c0py00046a

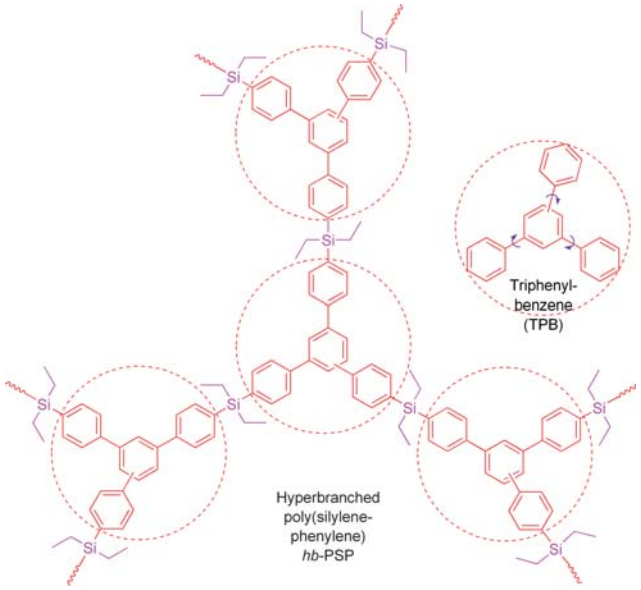

Chart 1 Structures of a σ*–π* conjugated *hb*-PSP and part of its repeat units TPB.

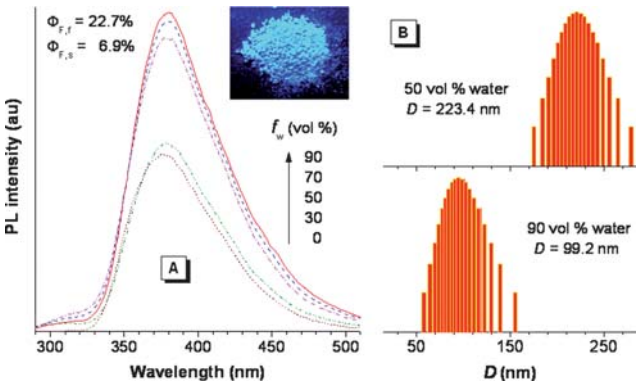

Fig. 2 (A) PL spectra of the *hb*-PSP in THF–water mixtures with different fractions of water (f_w). Inset: fluorescence image of the *hb*-PSP powder. (B) Size distributions of the nanoparticles of the *hb*-PSP aggregates suspended in the THF–water mixtures with f_w of 50 and 90 vol%; $\lambda_{ex} = 267$ nm; $c = 35$ μM.

Thus, when water is added into a THF solution of the *hb*-PSP, nanoaggregates of the polymer are formed and its photoluminescence (PL) is enhanced (Fig. 2A). The PL intensity is gradually increased with increasing water fraction (f_w) in the THF–water mixture, with its spectral profile remaining unchanged. Evidently, the polymer shows an aggregation-enhanced emission (AEE) effect.[6] Particle size analyses confirm the existence of the polymer nanoparticles with average sizes of ~223 and ~99 nm in the aqueous mixtures with 50 and 90 vol% water fractions, respectively (Fig. 2B). Fluorescence quantum yield of a solid film of the polymer ($\Phi_{F,f} = \sim 23\%$) is much higher than that of its THF solution ($\Phi_{F,s} = \sim 7\%$), further verifying its AEE effect.

In addition to being readily processable and thermally stable,[5] the *hb*-PSP possesses a 3D topological structure with numerous molecular cavities or voids for analyte capturing and diffusion pathways for exciton migration[7] as well as a very large band-gap energy with

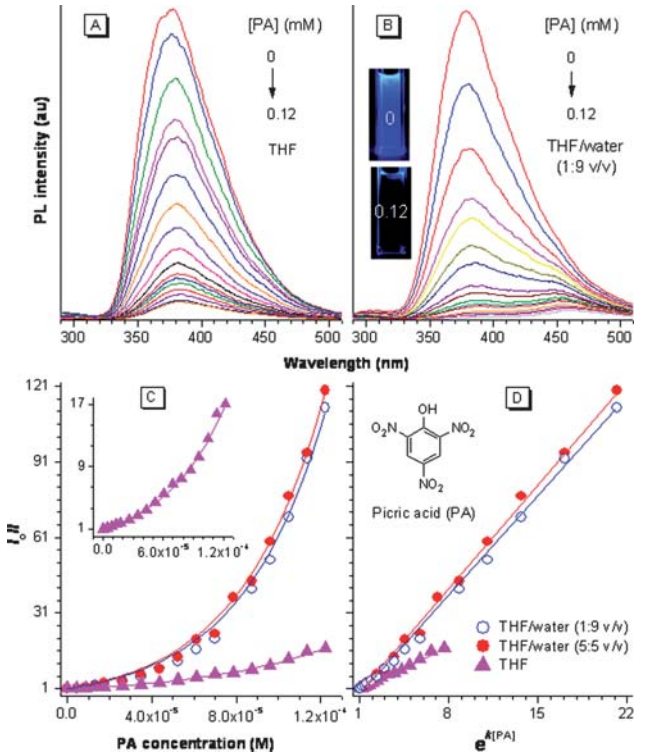

Fig. 3 Changes in the PL spectra of the *hb*-PSP with the addition of different amounts of PA in (A) THF solution and (B) THF–water mixture (1 : 9 v/v); $\lambda_{ex} = 267$ nm; $c = 35$ μM. Inset in panel B: fluorescence images of the *hb*-PSP in the THF–water mixture (1 : 9 v/v) with [PA] of 0 and 0.12 mM. (C) Stern–Volmer plots of I_0/I *versus* [PA] in THF and THF–water mixtures with f_w of 50 and 90 vol %; data for the aqueous mixture with $f_w = 50$ vol% taken from Fig. S2 (ESI);† I_0 = PL intensity in the absence of PA. Inset: enlarged plot in the THF solution. (D) Plots of I_0/I *versus* $e^{k[PA]}$ in THF solution and THF–water mixtures (5 : 5 and 1 : 9 v/v).

a deep-blue emission (ESI, Fig. S1).† The polymer is thus expected to work as an excellent fluorescent sensor for the detection of electron-deficient quenchers such as nitroaromatic explosives.[8] In this work, we used picric acid (PA) as a model explosive, because of its commercial availability. The quenching processes of the PL of the polymer were studied by monitoring its PL changes in response to the PA addition.

The PL spectrum of the *hb*-PSP is progressively weakened when an increasing amount of PA is added into its solution in THF or its nanoaggregates in the aqueous mixture (Fig. 3). The PL quenching can be clearly discerned at a PA concentration as low as 1 ppm. The PL intensity of the aggregates of the polymer suspended in the aqueous mixture decreases at a much faster rate than its isolated molecules dissolved in THF solvent. When the PA concentration is increased to 0.12 mM, virtually no light is emitted from the polymer nanoaggregates in the 90% aqueous mixture, as can be seen from the fluorescence image shown in Fig. 3B.

The Stern–Volmer plot of relative PL intensity (I_0/I) *versus* PA concentration in the THF solution gives a curve bending upward, instead of a linear line (Fig. 3C). Similar curves are obtained for the polymer nanoaggregates suspended in the aqueous mixtures with 50 and 90 vol% water content. A possible reason for the *hb*-PSP luminogen to give nonlinear Stern–Volmer plots is that the PL

annihilation is caused by static quenching or simultaneous dynamic and static quenching.[9]

For diffusion-controlled dynamic quenching, eqn (1) and (2) can be used to describe the quenching process:

$$\frac{\tau_0}{\tau} = \tau_0 k_q[\mathrm{PA}] + 1 \quad (1)$$

or

$$\frac{I_0}{I} = K_D[\mathrm{PA}] + 1 \quad (2)$$

where I_0 and I are the PL intensities and τ_0 and τ are the lifetimes of the polymer in the absence and presence of the PA quencher, respectively, k_q is the observed rate constant for the diffusion-controlled bimolecular quenching reaction, and K_D is the dynamic quenching constant and is equal to $\tau_0 k_q$.[9] The PL quenching by the static mechanism, on the other hand, can be described by the ground-state non-emissive fluorophore–quencher complex model (eqn (3)) or effective quenching sphere model (eqn (4)):

$$\frac{I_0}{I} = K_S[\mathrm{PA}] + 1 \quad (3)$$

$$\frac{I_0}{I} = e^{V_q[\mathrm{PA}]} \quad (4)$$

where K_s and V_q denote the static quenching constants in the complex and sphere models, respectively.[9] Eqn (3) can be viewed as an approximation of eqn (4) when PA concentration or V_q is very small. For the case of simultaneous dynamic and static quenching, eqn (5) and (6) are derived:

$$\frac{I_0}{I} = (K_D[\mathrm{PA}] + 1)(K_S[\mathrm{PA}] + 1) \quad (5)$$

$$\frac{I_0}{I} = (K_D[\mathrm{PA}] + 1)e^{V_q[\mathrm{PA}]} \quad (6)$$

One way to determine whether the quenching mechanism is dynamic, static or both of them is to measure the lifetimes of the luminogen in the absence and presence of the quencher.[9] If the quencher molecules are not bound to the luminogen molecules, the diffusion-controlled dynamic quenching will come into play as an additional non-radiative relaxation pathway and the lifetime of the luminogen will become shorter. In the static quenching, the luminogen molecules bound to the quencher molecules are in the non-emissive or "dark" state and the unbound ones exhibit their intrinsic lifetimes. As shown in Table 1 and Fig. S3 (ESI),† the weighted mean lifetimes of the *hb*-PSP remain almost unchanged when different amounts of PA are added, suggesting that the PL quenching is through a static mechanism or in other words, K_D in eqn (2) is practically zero. Accordingly, eqn (4) is more applicable to our system.

Table 1 Fluorescence decay parameters of the *hb*-PSP in THF at 380 nm in the presence of different amounts of PA[a]

No.	[PA]/10^{-5} M	A_1 (%)	A_2 (%)	τ_1/ns	τ_2/ns	$<\tau>$/ns[b]
1	0	60	40	0.16	1.95	0.88
2	2.6	60	40	0.15	1.83	0.82
3	5.2	65	35	0.16	2.01	0.81
4	7.8	68	32	0.17	2.17	0.81
5	10.4	67	33	0.17	2.21	0.84

[a] Determined from $I = A_1\exp(-t/\tau_1) + A_2\exp(-t/\tau_2)$, where A and τ are the fractional amount and PL lifetime of the shorter (1)- and longer (2)-lived species, respectively; concentration of polymer: 35 μM. [b] Weighted mean lifetime determined from $<\tau> = (A_1\tau_1 + A_2\tau_2)/(A_1 + A_2)$.

The *hb*-PSP possesses a 3D topological structure with a rigid aromatic scaffold. It contains many molecular cavities capable of capturing small PA molecules through electrostatic interaction or charge-transfer complexation, noting that the polymer (*hb*-PSP) is electron-rich while the quencher (PA) is electron-deficient. When the PA molecules are located inside a sphere with a volume V_q (effective quenching sphere) surrounding the polymer branches, the PL quenching is assumed to be completed. By fitting the Stern–Volmer plots shown in Fig. 3C, eqn (7)–(9) are obtained for the *hb*-PSP in the THF solution and in the aqueous mixtures with 50 and 90 vol % water contents, respectively. Generalization from eqn (7)–(9) furnishes eqn (10), which is different from the widely used eqn (4) by having two extra constants A and B, although they are both single exponential growth functions.

$$\frac{I_o}{I} = 2.4e^{16667[\mathrm{PA}]} - 1.4 \quad (7)$$

$$\frac{I_o}{I} = 5.8e^{25000[\mathrm{PA}]} - 4.8 \quad (8)$$

$$\frac{I_o}{I} = 5.4e^{25000[\mathrm{PA}]} - 4.4 \quad (9)$$

$$\frac{I_o}{I} = Ae^{k[\mathrm{PA}]} + B \quad (10)$$

Actually, eqn (10) is a more general one, because eqn (4) can be regarded as a special case of eqn (10) when A and B equal to 1 and 0, respectively. If we conservatively neglect the two constants A and B, the k values in eqn (7)–(9) becomes the static quenching constants. The constants (16667–25000 L mol^{-1}) are much higher than those (1–185 L mol^{-1}) of the well studied linear iptycene-containing poly(*p*-phenylenebutadiynylene)s and poly(*p*-phenyleneethynylene)s.[10] This enhanced amplification is easy to understand: in comparison to the 1D exciton migration along the linear polymer chains, the *hb*-PSP spheres afford multi-dimensional transport pathways for exciton to migrate. When the PA concentration is very small, eqn (10) is readily converted to eqn (11) by a mathematical treatment of Taylor expansion, which can be reorganized to give eqn (12), where $K = Ak$, $C = A + B = 1$.

$$\frac{I_0}{I} = A\left(1 + k[\mathrm{PA}] + \frac{1}{2}k^2[\mathrm{PA}]^2 + \cdots + \frac{k^n[\mathrm{PA}]^n}{n!} + \cdots\right) + B \quad (11)$$

$$\frac{I_o}{I} = A(1 + k[\mathrm{PA}]) + B = Ak[\mathrm{PA}] + A + B = K[\mathrm{PA}] + C \quad (12)$$

It becomes clear now that the static quenching constants (K) at the initial stage of the Stern–Volmer plots are 40000, 145000 and 135000 L mol^{-1} for the *hb*-PSP in the THF solution and in the THF–water mixtures with f_w of 50 and 90 vol%, respectively, which are much higher than those (K < 20000 L mol^{-1}) of the fluorescent chemosensors based on the linear polysiloles.[8] It is noteworthy that the quenching constant is dramatically increased from the solution

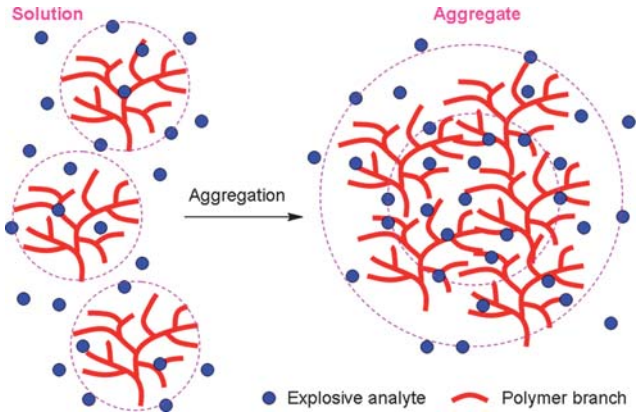

Fig. 4 Illustration of explosive detection by AEE-active *hb*-PSP in solution and aggregate states.

state to the nanoaggregate state, with the latter showing a remarkable superamplification effect.

Generally, intrinsic autoaggregation of FCP chains and/or their analyte-induced aggregation cause self-quenching problems that greatly reduce the sensing performance. However, aggregation is beneficial to the PL of the *hb*-PSP. Moreover, its aggregates have more cavities to bind with more quencher molecules and provide additional interbranch diffusion pathways for excitons to migrate (Fig. 4). The PA molecules in the inner cores and on the outer shells of the aggregates work cooperatively to facilitate the PL annihilation *via* electron and/or energy transfers, thus making the quenching a highly efficient process.

The aggregate-based sensor in the aqueous mixture with $f_w = 50\%$ shows a higher sensitivity than that with $f_w = 90\%$, probably because the polymer packing in the former is looser than in the latter and the looser packing allows more PA molecules to enter into the cavities. By plotting the relative PL intensities I_0/I *versus* $e^{k[PA]}$, linear lines are obtained in all the cases (Fig. 3D), which enables quantitative analysis. We are now conducting systematic studies of fabricating thin film-based chemosensor devices and examining their sensitivity and selectivity to different explosives.

In summary, in this work, we have developed a new, efficient chemosensor system for explosive detection operating in a static quenching mechanism. In comparison to linear FCPs, the *hb*-PSP possesses a 3D globular structure, which offers more diffusional channels for the excitons to migrate, allowing them to be quickly annihilated by the PA quenchers. Because of the AEE nature of the polymer, its aggregates do not suffer from the false-positive effect but show an enhanced sensing performance. The polymer nanoaggregates offer more cavities for the explosive molecules to enter and to interact with the chromophores, thanks to the loose packing of the polymer branches and the additional diffusional pathways. These advantageous structural features endow the *hb*-PSP nanoaggregates with a superamplification effect in the explosive detection process, as reflected by the very high static quenching constants (K up to 1.45×10^5 L mol^{-1}). We are now exploring this conceptually new type of extremely sensitive chemosensor for a wide range of high-tech applications.

This work was partially supported by the Research Grants Council of Hong Kong (603509 and 603008), the University Grants Committee of Hong Kong (AoE/P-03/08) and the National Science Foundation of China (20634020 and 20974028). B.Z.T. thanks the support from Cao Gaungbiao Foundation of Zhejiang University.

Notes and references

1 (*a*) S. W. Thomas III, G. D. Joly and T. M. Swager, *Chem. Rev.*, 2007, **107**, 1339; (*b*) U. H. F. Bunz, *Chem. Rev.*, 2000, **100**, 1605.
2 (*a*) Y. Liu, R. C. Mills, J. M. Boncella and K. S. Schanze, *Langmuir*, 2001, **17**, 7452; (*b*) H. M. Huang, K. M. Wang, D. Xiao, R. H. Yang and X. H. Yang, *Anal. Chim. Acta*, 2001, **439**, 55; (*c*) C. P. Chang, C. Y. Chao, J. H. Huang, A. K. Li, C. S. Hsu, M. S. Lin, B. R. Hsieh and A. C. Su, *Synth. Met.*, 2004, **144**, 297; (*d*) T. H. Kim, H. J. Kim, C. G. Kwak, W. H. Park and T. S. Lee, *J. Polym. Sci., Part A: Polym. Chem.*, 2006, **44**, 2059; (*e*) I. A. Levitsky, W. B. Euler, N. Tokranova and A. Rose, *Appl. Phys. Lett.*, 2007, **90**, 041904; (*f*) J. C. Sanchez and W. C. Trogler, *J. Mater. Chem.*, 2008, **18**, 3143; (*g*) T. Naddo, Y. Che, W. Zhang, K. Balakrishnan, X. Yang, M. Yen, J. Zhao, J. S. Moore and L. Zhang, *J. Am. Chem. Soc.*, 2007, **129**, 6978; (*h*) M. E. Germain and M. J. Knapp, *J. Am. Chem. Soc.*, 2008, **130**, 5422; (*i*) A. D. Hughes, I. C. Glenn, A. D. Patrick, A. Ellington and E. V. Anslyn, *Chem.–Eur. J.*, 2008, **14**, 1822; (*j*) Y. Jiang, H. Zhao, N. Zhu, Y. Lin, P. Yu and L. Mao, *Angew. Chem., Int. Ed.*, 2008, **47**, 8601; (*k*) K. Shiraishi, T. Sanji and M. Tanaka, *ACS Appl. Mater. Interfaces*, 2009, **1**, 1379; (*l*) Y. Long, H. Chen, Y. Yang, H. Wang, Y. Yang, N. Li, K. Li, J. Pei and F. Liu, *Macromolecules*, 2009, **42**, 6501.
3 (*a*) Y. Hong, J. W. Y. Lam and B. Z. Tang, *Chem. Commun.*, 2009, 4332; (*b*) J. Liu, J. W. Y. Lam and B. Z. Tang, *J. Inorg. Organomet. Polym. Mater.*, 2009, **19**, 249; (*c*) Z. Zhao, Z. Wang, P. Lu, C. Y. K. Chan, D. Liu, J. W. Y. Lam, H. H. Y. Sung, I. D. Williams, Y. Ma and B. Z. Tang, *Angew. Chem., Int. Ed.*, 2009, **48**, 7608; (*d*) J. Luo, Z. Xie, J. W. Y. Lam, L. Cheng, H. Chen, C. Qiu, H. S. Kwok, X. Zhan, Y. Liu, D. Zhu and B. Z. Tang, *Chem. Commun.*, 2001, 1740; (*e*) W. Z. Yuan, P. Lu, S. Chen, J. W. Y. Lam, Z. Wang, Y. Liu, H. S. Kowk, Y. Ma and B. Z. Tang, *Adv. Mater.*, 2010, **22**, DOI: 10.1002/adma.200904056.
4 (*a*) J. Liu, J. W. Y. Lam and B. Z. Tang, *Chem. Rev.*, 2009, **109**, 5799; (*b*) M. Häußler and B. Z. Tang, *Adv. Polym. Sci.*, 2007, **209**, 1.
5 J. Liu, R. Zheng, Y. Tang, M. Häußler, J. W. Y. Lam, A. Qin, M. Ye, Y. Hong, P. Gao and B. Z. Tang, *Macromolecules*, 2007, **40**, 7473.
6 Q. Zeng, Z. Li, Y. Dong, C. Di, A. Qin, Y. Hong, Z. Zhu, C. K. W. Jim, G. Yu, Q. Li, Z. Li, Y. Liu, J. Qin and B. Z. Tang, *Chem. Commun.*, 2007, 70.
7 S. Zahn and T. M. Swager, *Angew. Chem., Int. Ed.*, 2002, **41**, 4225.
8 (*a*) J. C. Sanchez, A. G. DiPasquale, A. L. Rheingold and W. C. Trogler, *Chem. Mater.*, 2007, **19**, 6459; (*b*) H. Sohn, M. J. Sailor, D. Magde and W. C. Trogler, *J. Am. Chem. Soc.*, 2003, **125**, 3821.
9 B. Valeur, *Molecular Fluorescence: Principle and Applications*, Wiley-VCH, Weinheim, 2002.
10 D. Zhao and T. M. Swager, *Macromolecules*, 2005, **38**, 9377.